

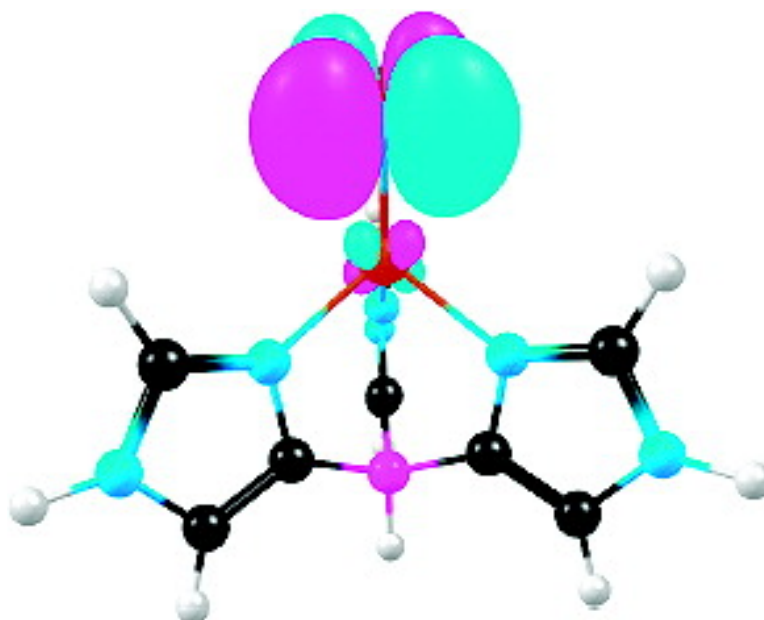
Communication

Modeling Side-On NO Coordination to Type 2 Copper in Nitrite Reductase: Structures, Energetics, and Bonding

Ingar H. Wasbotten, and Abhik Ghosh

J. Am. Chem. Soc., **2005**, 127 (44), 15384-15385 • DOI: 10.1021/ja0559909 • Publication Date (Web): 12 October 2005

Downloaded from <http://pubs.acs.org> on March 25, 2009



More About This Article

Additional resources and features associated with this article are available within the HTML version:

- Supporting Information
- Links to the 7 articles that cite this article, as of the time of this article download
- Access to high resolution figures
- Links to articles and content related to this article
- Copyright permission to reproduce figures and/or text from this article

[View the Full Text HTML](#)



ACS Publications
High quality. High impact.

Modeling Side-On NO Coordination to Type 2 Copper in Nitrite Reductase: Structures, Energetics, and Bonding

Ingar H. Wasbotten and Abhik Ghosh*

Department of Chemistry, University of Tromsø, N-9037 Tromsø, Norway

Received September 7, 2005; E-mail: abhik@chem.uit.no

Recent crystallographic studies by Murphy¹, Hasnain,² and their co-workers have led to major insights into the mechanism of copper nitrite reductase (CuNIR), one of two bacterial enzymes (the other being a heme nitrite reductase) that reduce nitrite to NO.^{3–5} The key new result consists of high-resolution CuNIR crystal structures with side-on NO coordination to the catalytically active type 2 copper, which is a unique structural motif in copper coordination chemistry. Though rare, side-on NO coordination has been previously observed, for example, in the photoisomer of a {RuNO}⁶ porphyrin, which has been characterized by low-temperature IR spectroscopy.⁶ In the case of the CuNIR, a key unresolved issue concerns the oxidation state—{CuNO}¹⁰ or {CuNO}¹¹—of this intermediate, where the superscripts refer to the Enemark–Feltham electron counts, namely, the number of metal d plus NO π^* electrons. We present here a DFT (PW91/TZP) study of side-on NO coordination for type 2 Cu model complexes as well as a reexamination⁷ of Ru(P)(NO)Cl (P = porphyrin, C_s , $S = 0$,^{8,9}

Side-on Ru(P)(NO)Cl, which is about 1.23 eV higher in energy than the end-on isomer,⁷ exhibits a quite unsymmetrical RuNO unit, with markedly unequal Ru–N_{NO} (2.0 Å) and RuO (2.4 Å) distances, as shown in Figure 1. Figure 1 also shows the three primarily Ru 4d-based MOs. Note that while the HOMO-4 depicts the main source of bonding between the a' Ru d_{π} orbital and the a' π^* orbital of the side-on NO, the HOMO-2 exhibits π -bonding between the Ru a'' d_{π} orbital and the nitrogen end of the a'' NO π^* orbital. The latter orbital interaction accounts for the unsymmetrical geometry of the side-on RuNO unit.

To model the CuNIR side-on NO intermediate, we have used the following supporting ligands: hydrotris(pyrazolyl)borate (HBpz₃⁻), hydrotris(4-imidazolyl)borate (HBim₃⁻), and tris(2-imidazolyl)methane (HCim₃). Remarkably, not only do the {CuNO}¹⁰ species exhibit metastable side-on isomers but so do the {CuNO}¹¹ species, which is unprecedented for Enemark–Feltham counts other than 6^{5,10} or 10.¹¹ For these three supporting ligands (in the above order), the energies of the side-on isomer, relative to the end-on isomers, are 0.52, 0.47, and 0.60 eV for {CuNO}¹⁰ and 0.29, 0.23, and -0.04 eV for {CuNO}¹¹. Thus, compared with side-on Ru(P)(NO)Cl,⁷ certain ones of the side-on CuNO isomers have remarkably low energies, and in one {CuNO}¹¹ case, the side-on geometry is actually preferred! On the basis of these results, therefore, the observed CuNIR intermediate may well be a ground state (as opposed to a metastable) species.

Figure 2 depicts the optimized geometries for Cu(HBpz₃)(η^1 -NO) and for [Cu(HBim₃)(η^2 -NO)]⁰⁺. Key features of the optimized geometry are in good agreement with a crystal structure of Cu[HB(3-*t*Bu-pz)₃](η^1 -NO).^{12–14} Figure 2 also shows that while the {CuNO}¹⁰ core is quite unsymmetrical (Cu–N_{NO} 1.9 Å, Cu–O 2.4 Å), the {CuNO}¹¹ core is much more symmetrical (Cu–N_{NO}

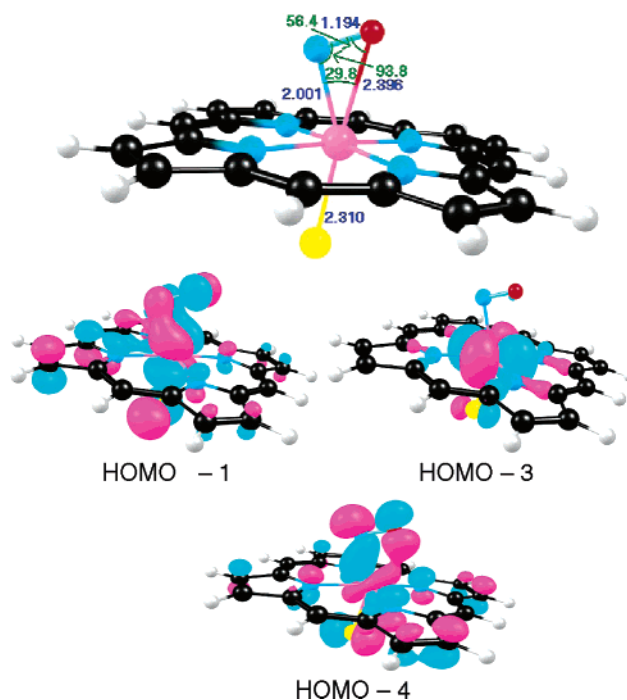


Figure 1. Ru(P)(η^2 -NO)Cl geometry (Å, deg) and MOs.

1.9 Å, Cu–O 2.1 Å). The latter geometry seems to be more in accord with experimental Cu–N/O distances reported for the CuNIR intermediate.^{1,2} On a more detailed note, the calculated Cu–N/O distances for the {CuNO}¹¹ core are closer to those found in ref 1 (2.0 Å) than in ref 2 (2.2 Å).

The MOs for analogous {CuNO}¹⁰ and {CuNO}¹¹ complexes are reasonably similar, although the former is $S = 0$ and the latter $S = 1/2$. For simplicity, Figure 3 shows an MO energy level diagram for Cu(HBim₃)(η^2 -NO), using a C_s symmetry-constrained spin-restricted calculation. (The more rigorous but larger spin-unrestricted diagram conveys essentially the same information.) As in the case of side-on Ru(P)(NO)Cl, note from Figure 3 that the bonding between Cu and the side-on NO ligand is mediated by an a' Cu(d_{π})–NO(π^*) orbital interaction. For Cu(HBim₃)(η^2 -NO), note that the Mulliken spin populations, the spin density plot (Figure 2), and a plot of the singly occupied MO (Figure 3) all indicate that the unpaired electron essentially occupies an NO a'' π^* orbital.

For the {Cu(η^2 -NO)}¹⁰ species, a spin-unrestricted (broken symmetry) calculation yields the same solution as a spin-restricted calculation, as opposed to an electronic structure involving metal–NO antiferromagnetic coupling. (However, we are aware that hybrid functionals may result in a somewhat different electronic description, compared with what we have found here.) For the

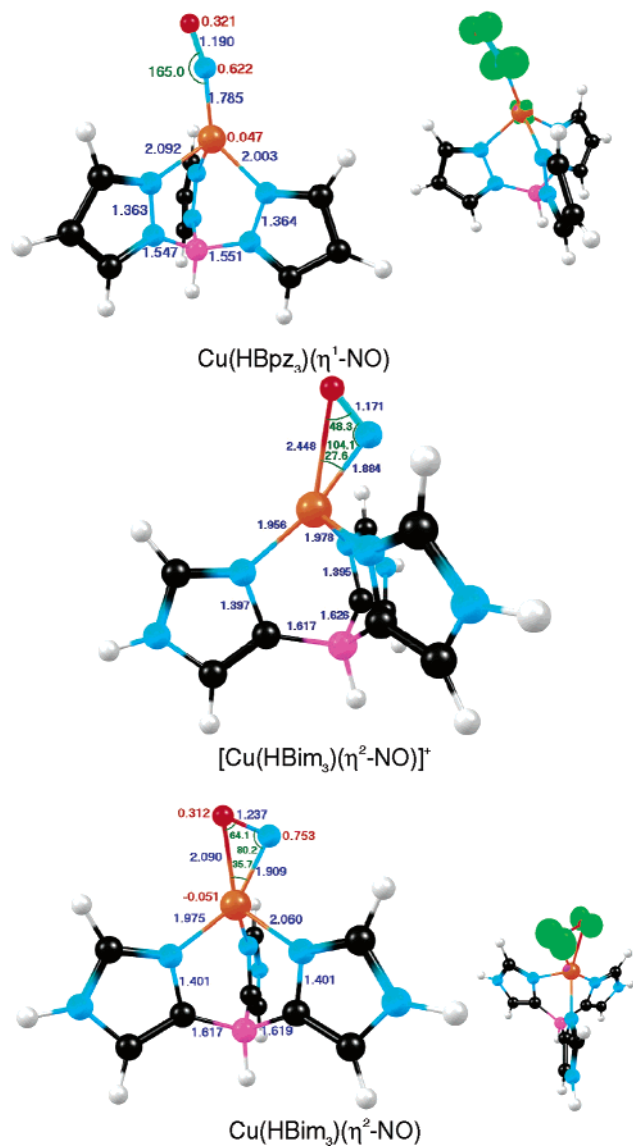


Figure 2. Distances (Å, blue), angles (deg, green), spin populations (red), and spin density plots (green).

{Cu(η^2 -NO)}¹¹ species, the spin density profile described above suggests an overall Cu^I-NO^{*} electronic description, rather than a tightly antiferromagnetically coupled Cu^{II}-NO⁻ formulation. Moreover, the latter description would have resulted in a large deviation of the calculated expectation value of \hat{S}^2 from the theoretically expected value of 0.75, which we do not observe; the calculated value of $\langle \hat{S}^2 \rangle$ is 0.76, in excellent agreement with the expected value.

In summary, PW91/TZP calculations indicate that both {CuNO}¹⁰ and {CuNO}¹¹ species may exhibit metastable side-on NO linkage isomers. However, the side-on isomers seem to be especially favored for the reduced $S = 1/2$ {CuNO}¹¹ oxidation level, where in one case, we found the side-on form to be actually more stable than the end-on form (albeit by a small margin). Indeed, it should be a worthwhile goal for synthetic inorganic chemists to attempt the synthesis of side-on {CuNO}¹¹ species. Moreover, the relatively symmetrical structure of the side-on {CuNO}¹¹ unit seems to be

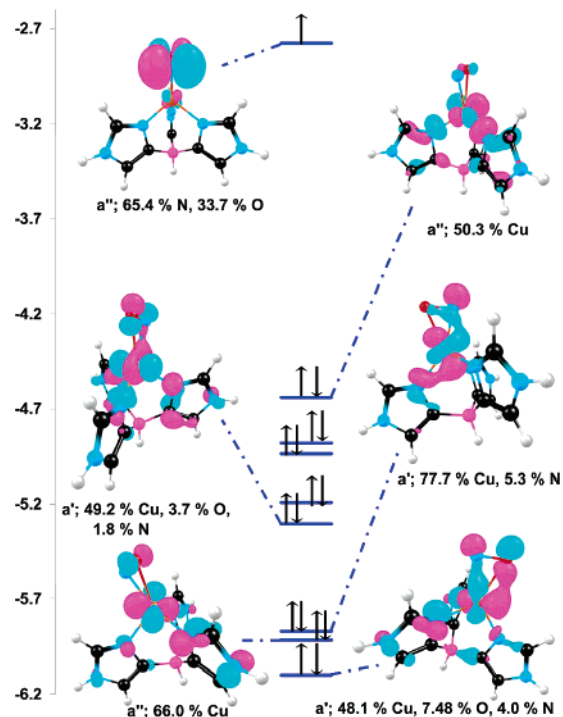


Figure 3. Energy level (eV) diagram for Cu(HBim₃)(η^2 -NO).

more consistent with the observed metrical parameters for the CuNIR intermediate.^{1,2}

Acknowledgment. This work was supported by grants from the Research Council of Norway.

Supporting Information Available: Optimized Cartesian coordinates are available. This material is available free of charge via the Internet at <http://pubs.acs.org>.

References

- (1) Tocheva, E. I.; Rosell, F. I.; Mauk, A. G.; Murphy, M. E. P. *Science* **2004**, *304*, 867.
- (2) Antonyuk, S. V.; Strange, R. W.; Sawers, G.; Eady, R. R.; Hasnain, S. S. *Proc. Natl. Acad. Sci. U.S.A.* **2005**, *102*, 12041.
- (3) Averill, B. A. *Chem. Rev.* **1996**, *96*, 2951–2964.
- (4) Farmer, P. J.; Sulc, F. J. *Inorg. Biochem.* **2005**, *99*, 166–184.
- (5) Wyllie, G. R. A.; Scheidt, W. R. *Chem. Rev.* **2002**, *102*, 1067–1090.
- (6) Fomitchev, D. V.; Coppens, P.; Li, T. S.; Bagley, K. A.; Chen, L.; Richter-Addo, G. B. *Chem. Commun.* **1999**, 2013.
- (7) Wondimagegn, T.; Ghosh, A. *J. Am. Chem. Soc.* **2001**, *123*, 5680–5683.
- (8) Unless otherwise mentioned, all calculations described here are spin-unrestricted. All calculations used the PW91 functional for both exchange and correlation and Slater-type triple- ζ plus polarization basis sets, as implemented in the ADF program system.
- (9) For recent DFT calculations on transition metal nitrosyls from our laboratory, see: (a) Ghosh, A.; Wondimagegn, T. *J. Am. Chem. Soc.* **2000**, *122*, 8101–8102. (b) Conradie, J.; Wondimagegn, T.; Ghosh, A. *J. Am. Chem. Soc.* **2003**, *125*, 4968–4969. (c) Review: Ghosh, A. *Acc. Chem. Res.* In press.
- (10) Side-on nitroprusside: Carducci, M. D.; Pressprich, M. R.; Coppens, P. *J. Am. Chem. Soc.* **1997**, *119*, 2669–2678.
- (11) Side-on Cp^{*}NiNO: Fomitchev, D. V.; Furlani, T. R.; Coppens, P. *Inorg. Chem.* **1998**, *37*, 1519–1526.
- (12) Schneider, J. L.; Carrier, S. M.; Ruggiero, C. E.; Young, V. G.; Tolman, W. B. *J. Am. Chem. Soc.* **1998**, *120*, 11408–11418.
- (13) Ruggiero, C. E.; Carrier, S. M.; Antholine, W. E.; Whittaker, J. W.; Cramer, C. J.; Tolman, W. B. *J. Am. Chem. Soc.* **1993**, *115*, 11285–11298.
- (14) Carrier, S. M.; Ruggiero, C. E.; Tolman, W. B.; Jameson, G. B. *J. Am. Chem. Soc.* **1992**, *114*, 4407–4408.

JA0559909